The Journal of Experimental Biology 214, 1283-1293

doi:10.1242/jeb.050427

## RESEARCH ARTICLE

# Ocellar adaptations for dim light vision in a nocturnal bee

Richard P. Berry[1], William T. Wcislo[2] and Eric J. Warrant[3,*]

[1]Centre for Visual Sciences, School of Biology, Australian National University, Canberra 2600, Australia, [2]Smithsonian Tropical Research Institute, Apartado 2072, Balboa, Republic of Panama and [3]Department of Cell and Organism Biology, University of Lund, Sölvegatan 35, Lund S-22350, Sweden

*Author for correspondence (eric.warrant@cob.lu.se)

Accepted 20 December 2010

**SUMMARY**

**Growing evidence indicates that insect ocelli are strongly adapted to meet the specific functional requirements in the environment in which that insect lives. We investigated how the ocelli of the nocturnal bee *Megalopta genalis* are adapted to life in the dim understory of a tropical rainforest. Using a combination of light microscopy and three-dimensional reconstruction, we found that the retinae contain bar-shaped rhabdoms loosely arranged in a radial pattern around multi-layered lenses, and that both lenses and retinae form complex non-spherical shapes reminiscent of those described in other ocelli. Intracellular electrophysiology revealed that the photoreceptors have high absolute sensitivity, but that the threshold location varied widely between $10^9$ and $10^{11}$ photons cm$^{-2}$ s$^{-1}$. Higher sensitivity and greater visual reliability may be obtained at the expense of temporal resolution: the corner frequencies of dark-adapted ocellar photoreceptors were just 4–11 Hz. Spectral sensitivity profiles consistently peaked at 500 nm. Unlike the ocelli of other flying insects, we did not detect UV-sensitive visual pigments in *M. genalis*, which may be attributable to a scarcity of UV photons under the rainforest canopy at night. In contrast to earlier predictions based on anatomy, the photoreceptors are not sensitive to the *e*-vector of polarised light. *Megalopta genalis* ocellar photoreceptors possess a number of unusual properties, including inherently high response variability and the ability to produce spike-like potentials. These properties bear similarities to photoreceptors in the compound eye of the cockroach, and we suggest that the two insects share physiological characteristics optimised for vision in dim light.**

Supplementary material available online at http://jeb.biologists.org/cgi/content/full/214/8/1283/DC1

Key words: ocelli, bee, nocturnal vision, sensitivity, polarisation sensitivity, spectral sensitivity, response dynamics.

## INTRODUCTION

*Megalopta genalis* is a stick-dwelling bee that inhabits dense rain forest understories within Central and South America. *Megalopta genalis* is referred to as a nocturnal bee because it emerges to forage after dusk and before dawn, when light intensities under the forest canopy are approximately the equivalent of a starlit night above the rainforest canopy (Warrant et al., 2004; Kelber et al., 2006). At light intensities where little is visible to a human observer, *M. genalis* navigates through the rainforest understory, learns and visually orients to landmarks, and relocates its nest from a background of dense vegetation (Warrant et al., 2004; Wcislo et al., 2004) [for other dim-light bees and wasps, see Warrant and others (Warrant, 2008a; Warrant, 2008b; Wcislo and Tierney, 2009)].

The apposition compound eyes of *M. genalis* possess several adaptations to life in a dim environment. Compared with diurnal bees, the facets and rhabdoms of the eye are greatly enlarged (Greiner et al., 2004a; Kelber et al., 2006) and the photoreceptors have high gain and sensitivity (Frederiksen et al., 2008). There is also substantial anatomical and theoretical evidence to indicate that visual signals are spatially and temporally pooled at the later stages of visual processing, which improves sensitivity at the expense of spatial resolution (Greiner et al., 2004b; Greiner et al., 2005; Theobald et al., 2006; Theobald et al., 2007; Warrant, 2008a).

Bees, like many other insects, possess two visual pathways: the compound eyes, and an additional set (typically three) of single-lens eyes (ocelli). Variation in the number, form and location of the ocelli between insects has led to numerous and diverse proposals of ocellar function (reviewed in Goodman, 1981; Mizunami, 1994). Wilson proposed the most convincing hypothesis of ocellar function in flying insects to date (Wilson, 1978). His ‘single-sensor model’ (from Stange et al., 2002) suggested that each ocellus is optimised for detecting illumination levels, and together the ocelli act as a ‘rough and ready’ autopilot system for maintaining stability during flight with respect to pitch, yaw and roll. A simple system capable of correcting for flight instability is achieved by feeding the change in intensity measured by the three ocelli to wing motor neurons (Wilson, 1978). One would predict that such a system should be adapted for high sensitivity and speed, and indeed the ocelli are typically well adapted for these functions through a number of features such as low *F*-number lenses (Berry et al., 2007a; Berry et al., 2007b), high convergence ratios (Toh and Kuwabara, 1974; Patterson and Chappell, 1980), high synaptic gain (Simmons, 1995) and a low number of intervening synapses between ocellar photoreceptors and wing motor centres (Pan and Goodman, 1977; Guy et al., 1979; Simmons, 1980; Simmons, 1981; Simmons and Littlewood, 1989). Conversely, the ocelli should have little need for spatial resolution, and indeed the strongly underfocused ocellar lenses of many insects make them ill-adapted for form vision (Homann, 1924; Parry, 1947; Cornwell, 1955; Wilson, 1978; Schuppe and Hengstenberg, 1993; Warrant et al., 2006).

Following the development of the single-sensor hypothesis, ocellar-driven corrective responses of the type proposed by Wilson

(Wilson, 1978) were demonstrated behaviourally in dragonflies (Stange, 1981), locusts (Taylor, 1981) and bees (Kastberger, 1990). Recently, Parsons et al. have also demonstrated that the lobula plate tangential cells V1 and VS in the fly respond in a rotation-specific manner to stimulation of the ocelli, as well as to stimulation of the compound eye (Parsons et al., 2006; Parsons et al., 2010). The preferred direction of rotation to stimulation of the ocelli matches the preferred direction of rotation to stimulation of the compound eye, suggesting that the two visual systems interact in a synergistic fashion to encode rotation of the animal in space (Parsons et al., 2006; Parsons et al., 2010).

However, it is becoming increasingly clear that insect ocelli are adapted to fulfill particular requirements demanded by the lifestyle and environment in which the animal lives (Mizunami, 1995). Dragonfly ocelli, for example, have been shown to be optimally adapted for resolving the horizon itself, rather than changes in brightness during flight (Stange et al., 2002; Berry et al., 2006; Berry et al., 2007a; Berry et al., 2007c; van Kleef et al., 2008). Some capacity for perceiving form has also been demonstrated in the ocelli of locusts (Berry et al., 2007b) and wasps (Warrant et al., 2006), suggesting that their function may also be more complex than previously thought.

In a visually cluttered low-light environment where the horizon is not readily visible, how might the ocelli of *M. genalis* be adapted to serve a single-sensor function? Taxonomists have long known that nocturnal species of bees and wasps have particularly enlarged ocelli in comparison with their day-flying relatives (Kerfoot, 1967; Michener, 2000; Wcislo and Tierney, 2009). An earlier study by Warrant et al. (Warrant et al., 2006) found that the ocelli of *M. genalis* are especially strongly adapted for high sensitivity, with large ocellar lenses and an occupancy ratio (percentage area of the retina occupied by rhabdom) five times larger than in diurnal species, and three times larger than in another nocturnal insect, the wasp *Apoica pallens*. They also described the rhabdoms of *M. genalis* ocelli as elongated in shape, consisting of parallel microvilli aligned in a single direction, which strongly suggests the ability to detect the *e*-vector orientation of polarised light. Interestingly, polarisation-sensitive ocelli have been demonstrated in the bumblebee (Wellington, 1974) and the desert ant (Mote and Wehner, 1980), which led Warrant et al. (Warrant et al., 2006) to tentatively suggest that the ocelli of *M. genalis* could serve as a highly sensitive nocturnal polarisation compass. In the present study, we used intracellular electrophysiology to determine whether the ocellar photoreceptors of *M. genalis* are polarisation sensitive. We also determined the absolute sensitivity of the ocellar photoreceptors, the wavelengths of light that they are most sensitive to, and their temporal dynamics in low-light conditions. Physiology is supplemented by ocellar anatomy, using serial sectioning and three-dimensional reconstruction. We compare the results obtained from *M. genalis* to those known from the ocelli of other insects in order to determine characteristics likely to be specialised for ocellar function in the rainforest understory at night.

## MATERIALS AND METHODS

### Animals

All experiments were performed on the nocturnal halictid bee *Megalopta genalis* Meade-Waldo 1916. Bees were collected between 19 and 29 March 2008 from Barro Colorado Island, a tropical rainforest reserve in the Republic of Panama [for details of the site, see Leigh (Leigh, 1999)]. Adult bees were collected by light trapping at night on a white sheet illuminated with bright ultraviolet (UV) light. Additional adult and juvenile bees were obtained by collecting bee nests from the rainforest understory. Bees and nests were transported to Lund, Sweden, where they were kept at 22–24°C and ~65% humidity. Newly emerged bees were allowed to feed on a 1:1 solution of honey and water for 24 h. After this time, bees were placed in an 8°C refrigerator, which allowed storage of live bees for several days. Both bee nests and refrigerated bees were kept under a reversed 12 h:12 h light:dark cycle. The experiments described below were performed during the 12 h dark cycle, corresponding to their natural nocturnal behaviour. All experiments described here comply with laws regarding animal welfare in Panama, Sweden and Australia, where the work was performed.

### Histology

The ocelli of 10 female bees were examined by standard light microscopy procedures. Whole head capsules were exposed by making several incisions in the frons, cuticle and compound eyes in order to enhance fixative penetration. Bee heads were then fixed either by placing them in a solution of 2% formaldehyde and 2.5% glutaraldehyde in 0.15 mol $l^{-1}$ cacodylate buffer for 24 h, or by first submerging the head in 80°C water for 30 s, followed by fixation for 24 h. After fixation, samples were rinsed in buffer, postfixed in 1% phosphate buffered osmium tetroxide, dehydrated through a graded acetone series and embedded in Epon 812 resin (EMS, Hatfield, PA, USA). Semi-thin 1 μm sections of the ocelli were cut with a diamond knife (Diatome, HistoJumbo, Biel, Switzerland) on a Reichert-Jung ultramicrotome (Vienna, Austria). For viewing, sections were post-stained with Toluidine Blue and imaged on a Zeiss Axioplan 2 equipped with a Zeiss MRc camera (Carl Zeiss AB, Stockholm, Sweden).

### Three-dimensional reconstruction

One embedded specimen was selected for the generation of a three-dimensional reconstruction of the ocelli and surrounding structures. This specimen was serially sectioned at 1 μm intervals, with every tenth section retained and imaged on a Zeiss Axioplan 2 equipped with a Zeiss AxioVision Panorama module. This module allows multiple high-resolution images of different regions of a section to be stitched seamlessly together, creating a single high-resolution image. The dimensions of the entire reconstructed block were approximately 2.5×1.6×1.5 mm with voxel (μm $pixel^{-1}$) dimensions of 1.289×1.289×10 (width×height×depth).

The image stack was imported into Amira 3.1 (Visage Imaging, Richmond, VIC, Australia), where images were manually aligned to their best possible fit relative to each other. After alignment, each image was segmented into discrete components by manually tracing outlines of the ocellar lenses, ocellar retinae, brain and compound eyes. Mesh models of each structure were then generated from the segmented images. In order to reduce polygon count and smooth surfaces without a loss of structural detail, the original meshes were imported into Silo (Nevercenter, Salt Lake City, UT, USA) and used as bases over which new meshes were manually redrawn. To greatly facilitate this process, segmentation and redrawing were performed on one side of the bee only, with the opposing side generated by mirror copying.

### Electrophysiology

#### Preparation

A cold-anaesthetised bee was placed inside a small open-ended plastic tube, with its head firmly fixed to the rim of the tube with wax. All recordings were obtained from the retina of the median ocellus, which was exposed by cutting a small slit into the cuticle

just above the median lens, between the two lateral ocelli (black box in Fig. 1C). To prevent hardening of the haemolymph, the incision was immediately filled with Vaseline®. A thin silver chloride wire inserted into one of the compound eyes served as the indifferent electrode. The point of indifferent electrode insertion was also coated with Vaseline® to prevent dehydration. All experiments were performed during the bee's 'night state' (i.e. during the 12 h dark cycle).

### Intracellular recording

Fine tipped microelectrodes were pulled from thick-walled glass (Science Products, GB 100F-10, Hofheim, Germany) on a P-87 Flaming/Brown microelectrode puller (Novato, CA, USA). After backfilling with 1 mol $l^{-1}$ LiCl, electrodes typically had a DC resistance of 150–200 MΩ. The output from the electrode was passed through an amplifier (NPI Electronics, BA-03X, Tamm, Germany), filtered through a 50/60 Hz noise eliminator (Hum Bug, Quest Scientific, North Vancouver, BC, Canada), digitised (National Instruments data acquisition card, Austin, TX, USA) and stored on a PC running LabVIEW 7.1 (National Instruments).

After preparation, bees were placed into the centre of the electrophysiology setup with the dorsal surface facing upwards, and the median ocellus was tilted ~20 deg upwards from the horizontal. A microelectrode was positioned just above the slit exposing the median ocellar retina and was advanced until an ERG response to a flash of light was encountered. At that time, all lights were switched off and the bee was left to rest in the dark for 30 min. After the rest period, the microelectrode was advanced until a response to a light flash characteristic of an intracellular recording of an ocellar photoreceptor was encountered (Chappell and Dowling, 1972) (reviewed in Goodman, 1981). If the amplitude of response to a bright flash of white light was greater than 15 mV, the recording quality was deemed to be acceptable for further analysis.

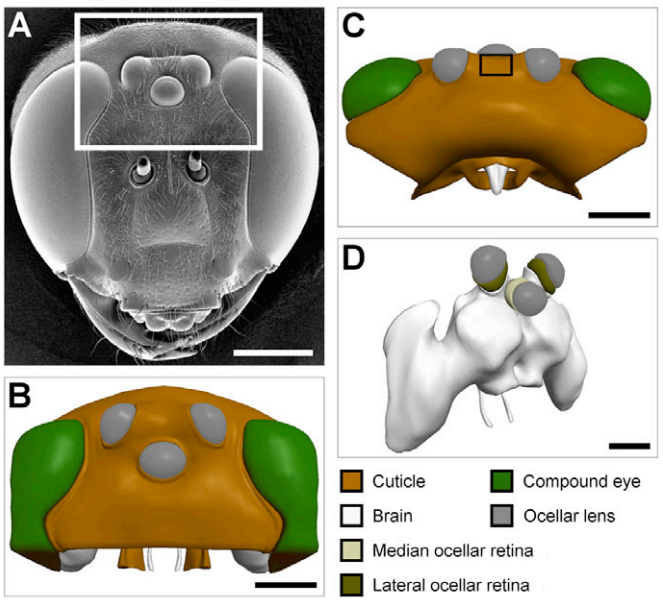


Fig. 1. Gross morphology and three-dimensional reconstruction of the ocelli of *Megalopta genalis*. (A) Scanning electron microscope image of the head (from Warrant et al., 2006). (B) Anterior view of the reconstructed ocelli and surrounding tissues. The area bounded by the white box in A indicates the approximate region of the head that was reconstructed in this study. (C) Dorsal view of the reconstructed ocelli and surrounding tissues. The black box indicates the location and size of the incision made in the cuticle during preparation for intracellular recording. (D) Oblique view of the brain, ocellar lenses and retinae. Scale bars, 500 μm.

### The stimulus

All stimuli were generated from a xenon arc lamp housed in a light-proof box in the same room as the experimental setup. Light from the lamp was collected and focused into a beam that passed through a series of filter blocks and shutters. Two filter blocks housed neutral density filters, which allowed stimulus intensity to be controlled over a total range of 6 log units in 0.2 log unit increments. The remaining filter blocks housed interference filters that allowed control of stimulus wavelength over a range of 330–700 nm in 10–20 nm intervals (bandwidth 8 nm). A mechanical shutter (UniBlitz T132, Rochester, NY, USA) allowed precise control of the duration of light flashes with 1 ms accuracy. Neutral density filters, interference filters and the mechanical shutter were controlled by a custom written program in LabVIEW 7.1, which allowed independent and semi-automated control of stimulus intensity, colour and duration.

After passing through the filter blocks and shutter, light was focused into a quartz fibre optic cable (diameter 100 μm), which carried light to the electrophysiology setup. The end of the fibre optic cable was mounted on a cardan arm with a rotation radius of 80 mm. The bee was positioned at the centre of the arm, such that the stimulating point light source (subtending 0.3 deg at the eye) could be moved to any position in azimuth or elevation around the head of the bee. An adaptor fitted to the end of the fibre optic cable also allowed a linear polarisation filter to be inserted in the light path. The filter could be manually rotated in 10 deg steps over a total range of 360 deg.

When an intracellular recording of an ocellar photoreceptor was obtained, the stimulus was moved around the head of the bee to the position that resulted in the maximum response amplitude. Responses to various predetermined regimes of light flashes were recorded for as long as a stable recording was maintained. Intensity-response functions were measured by determining the intensity of 500 nm light that elicited a visible response and then recording responses to flashes of successively increasing intensity. Intensity-response functions were obtained from 13 photoreceptors. Spectral sensitivity functions were determined by first determining the intensity of a 500 nm flash required to produce a response of ~50% of maximum amplitude and then recording responses to light flashes of the same intensity but different wavelength. Spectral sensitivity functions were obtained from nine photoreceptors. Polarisation sensitivity was determined by inserting a polarising filter into the light path and manually rotating the filter such that response amplitude to a flash of white light was maximised. An intensity-response function taken with the filter in this orientation (theoretical maximum) was compared with the succeeding intensity-response function taken with the filter rotated by 90 deg (i.e. theoretical minimum). Polarisation sensitivity was tested in this manner for three photoreceptors. For all stimuli described above, light flashes were 40 ms in duration, and three repeats of each measurement were taken (mean values of all three repeats were used for analysis). Long intervals were used between each flash (typically 15 s) to ensure that the photoreceptor remained in the dark-adapted state.

Impulse-response functions were obtained by stimulating a photoreceptor with a 2 ms long flash of white light of sufficient intensity to elicit a response of 2–3 mV in amplitude. Impulse-response functions were obtained from six photoreceptors. In this case, stimuli were delivered at an interval of 5 s between flashes,

and a total of 100 repeats were taken. The mean value of all 100 repeats was taken as the cell's impulse response.

### Data analysis and calibration

Recordings were analysed offline in a custom written MATLAB (The MathWorks, Natick, MA, USA) program. Initially, response strength to a given stimulus was taken as the maximum change in voltage between the resting membrane potential and the peak response. However, this approach proved unsuccessful because response waveform often changed rapidly with intensity. In particular, the sudden appearance of large-amplitude phasic responses or 'spike-like potentials' (see Fig. 3) often resulted in artificial peaks in the intensity-response and spectral sensitivity functions that did not correlate well with the cell's true sensitivity. To resolve this problem, high-frequency components were removed in software by low-pass filtering, and therefore only the low-frequency component of the response was used to determine the response amplitude to a given stimulus.

The constant intensity flash method was used to obtain photoreceptor spectral sensitivity functions. Voltage responses to stimuli of approximately constant quantal intensity at different wavelengths were recorded and then converted to sensitivity values by transformation through an intensity-response function taken with monochromatic light at the photoreceptor's peak response wavelength (500 nm was always used). Sigmoidal functions were fitted to the intensity-response functions, and solving these functions for $x$ yielded sensitivity values.

A disadvantage of the constant intensity method is that the spectrum of light emitted from a xenon arc lamp is not flat, but tends to be brighter at green wavelengths than at UV or red wavelengths. To compensate for this, a suitable neutral density filter was automatically inserted into the light path at each change of stimulus wavelength, so that the stimulus delivered at all wavelengths was approximately isoquantal. However, as the neutral density filters used in our setup varied in increments of 0.2 optical density units, some variation in intensity at different wavelengths remained. The resulting mismatch was taken into account by adding an offset factor when interpolating sensitivity values from intensity-response functions. This offset value corresponded to the difference between actual stimulus intensity and the theoretical intensity necessary to make all wavelengths of constant intensity. Actual stimulus intensities were determined by carefully measuring photon flux at each wavelength using an International Light IL1700 Research Radiometer (Peabody, MA, USA).

## RESULTS

### Histology and general morphology

The three ocelli of *M. genalis* bulge conspicuously from the dorsal surface of the head, between the two compound eyes. The median ocellus is the most ventral and is directed frontally whereas the two lateral ocelli sit further dorsally and laterally and are directed to the side and upwards (Fig. 1). In order to aid understanding of the morphology of the ocellar lenses and retina described in the following sections, an interactive three-dimensional model of the ocelli is presented in supplementary material Fig. S1.

### The ocellar lenses

As described by Warrant et al. (Warrant et al., 2006), the ocellar lenses are slightly elliptical, being wider in the horizontal direction than the vertical direction. As determined from longitudinal sections, the lateral ocelli are larger, with mean lens diameters of 424–446 μm compared with 385–440 μm in the median ocellus. Externally, the outer surfaces of the lenses appear strongly curved. On average, the median ocellus lens was flatter than the lateral ocellar lenses, with a radius of curvature (mean ± s.d.) of 604±168 μm compared with 466±48 μm, respectively. These curvatures are not sufficient to bring incoming light rays into focus on the retina (Warrant et al., 2006); *M. genalis* ocelli, like those of many other insects, are profoundly underfocused.

In this study, we found that the inner surfaces of the lenses of *M. genalis* form complex non-spherical shapes (supplementary material Fig. S1). The inner surface of the median ocellar lens is pinched inwards along the midline, resulting in a slightly bilobed shape (Fig. 2A). The inner surface is skewed such that the bulk of the lens projects dorsally. The inner surface of the lateral ocellar lens is similarly skewed, with the bulk of the lens projecting medially (Fig. 2B).

Sections through the lenses also revealed that each lens consists of at least three structurally distinct components (Fig. 2A,B). Exact boundaries between the three layers were often difficult to define, and it was not deemed to be feasible to reconstruct individual layers of the lens. The outer layer is the largest of the three layers and constitutes the majority of the lens. This layer is composed of consecutive layers of tissue that stain lightly with Toluidine Blue. The middle layer is similarly composed of tightly layered tissue. This layer, however, stains much more densely with Toluidine Blue. The inner layer is not composed of layered tissue and appears to be largely devoid of cellular structure. The gelatinous appearance of this layer suggests that it may represent a vitreous humour. However, the high density of staining with Toluidine Blue (Fig. 2A,C) indicates a high concentration of organic material. Further, the margins of the inner layer often appeared to be confluent with the lens. These factors suggest that this layer is a component of the lens itself rather than a vitreous humour. It is currently unclear whether the optical properties of each layer differ. Complex lens optics have, however, recently been described in the median ocellus of dragonflies (Berry et al., 2007a).

### Structure of the retina

The rhabdomeric zones of the retinae form layers 40–50 μm thick directly behind the inner surfaces of the lenses. The proximal limit of each rhabdom zone is marked by pigment, which accumulates along the edges of the retina (Fig. 2A,B). The rhabdomeric zone follows the inner shape of the lenses; thickening of the lens corresponds to thickening of the retina (e.g. Fig. 2B). Thus, the majority of the median ocellar retina projects in a dorsal direction (Fig. S1) whereas the lateral ocellar retinae are thicker medially than laterally (Fig. 2B, supplementary material Fig. S1). A particularly pronounced thickening of the retina is located at the dorsomedial extremes of the lateral ocelli.

In *M. genalis*, the ocellar rhabdoms are formed by the fusion of rhabdomeres of two adjacent photoreceptors with nearly parallel microvilli (Warrant et al., 2006). Each ocellus contains in the order of 150–200 rhabdoms, as ascertained by counting rhabdom profiles in cross-sections of the retinae. The rhabdoms are strongly elongated in one direction and narrow in the other (Fig. 2C,D); thus their three-dimensional shape resembles a thin ribbon-like strip. In distal cross-sections through the median retina, rhabdoms tend to form straight lines that are not aligned in a common direction, but rather form a loose radial pattern around the lens (Fig. 2C). In proximal cross-sections this pattern becomes less obvious and there is an increasing tendency for the rhabdoms to form irregular worm-like shapes (Fig. 2D).

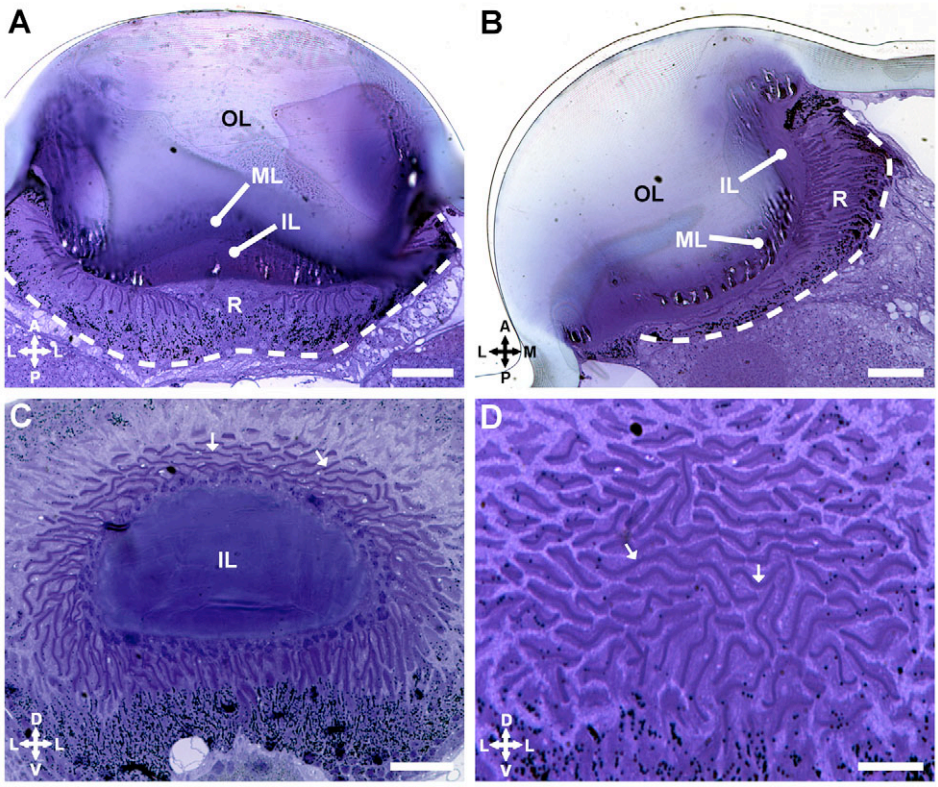


Fig. 2. Longitudinal and cross-sections of the ocelli of *M. genalis*. (A) Horizontal longitudinal section through the median ocellus. The lens consists of three ill-defined components: the outer layer (OL), middle layer (ML) and inner layer (IL). The rhabdomeric zone (R) begins directly behind the inner layer. Proximally, the rhabdoms are enclosed by a layer of dark pigment (dashed white line). (B) Horizontal longitudinal section through the left lateral ocellus. The lens and retina are thicker anteromedially than posterolaterally. (C) Cross-section through the base of the median ocellar lens and retina. Rhabdoms (examples at arrows) are loosely oriented in an irregular radial pattern around the lens. (D) High magnification cross-section through the median ocellar retina, 30 μm proximal to image shown in C. Rhabdoms (arrows) are generally worm-like in appearance. A, anterior; D, dorsal; L, lateral; M, medial; P, posterior; V, ventral. Scale bars, 50 μm (A–C), 20 μm (D).

### Electrophysiological responses

#### Responses to light pulses

Photoreceptors of *M. genalis* ocelli, like those of other insects (reviewed in Goodman, 1981), may respond to light stimulation with a fast graded 'on spike', a slower depolarising wave and a tonic depolarisation that is maintained for the length of the stimulus. In *M. genalis*, we found an especially wide range of response waveforms (Fig. 3). Comparing response waveforms between recordings was difficult because the same cell may respond quite differently to stimuli of different intensities. For example, the cell presented in Fig. 3A responded solely with slow depolarising waves to a low-intensity stimulus ($I$=–2.0), but at a marginally brighter intensity ($I$=–1.8) the response changed markedly to include multiple phasic peaks or 'spike-like' potentials riding the slow depolarisation. The appearance of spike-like potentials at a particular threshold was a common feature between photoreceptor recordings. However, the threshold intensity required to elicit these potentials varied widely between recordings, from ~0.78 to 2.44 log units above the intensity at which the smallest response was observed. In many recordings, no spike-like potentials were observed, and the light response at all intensities consisted only of a slow depolarisation. In other recordings, only a single phasic peak at the very beginning of the response was observed. The first spike-like potential was typically strongly graded with intensity; increasing intensity resulted in an

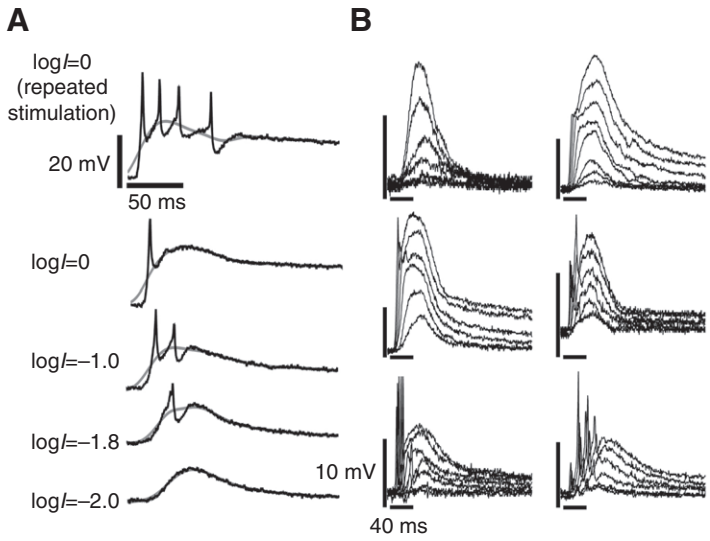


Fig. 3. Variation in response waveform to 40 ms square wave light flashes of varying intensity. (A) Raw and filtered responses from the same photoreceptor. Log$I$ indicates the intensity of the stimulus in log units below maximum possible intensity (log$I$=0). Black lines, raw responses; grey lines, low-pass filtered responses used to determine response amplitudes for intensity-response and spectral sensitivity functions. (B) Pulse responses of six different photoreceptors. Response waveform varies from entirely graded (top left) to dominated by spike-like potential (bottom right). Responses to various intensities are shown: the topmost trace is always brightest intensity; lower traces show responses to decreasing intensity in steps of –0.4 log units (log$I$=0, –0.4, –0.8, –1.2, etc.).

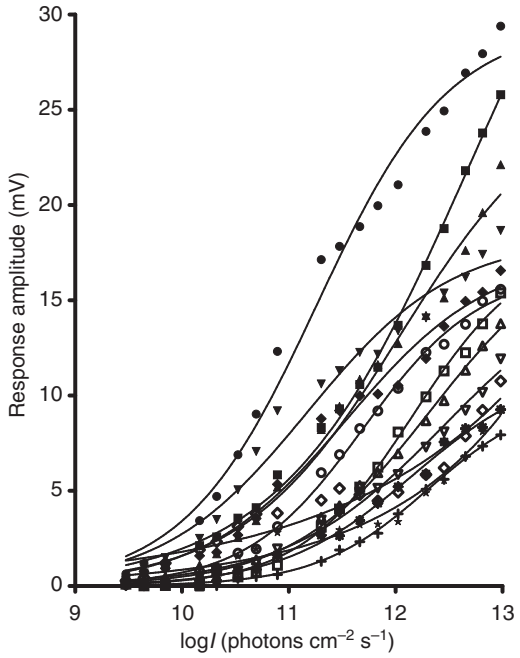


Fig. 4. Intensity-response functions recorded from 13 ocellar photoreceptors (represented by different symbols) in *M. genalis*. Functions were determined from responses to an axial point source emitting green (500 nm) light. Intensity-response functions are widely shifted along the abscissa, but in no case was the saturation point reached with monochromatic light.

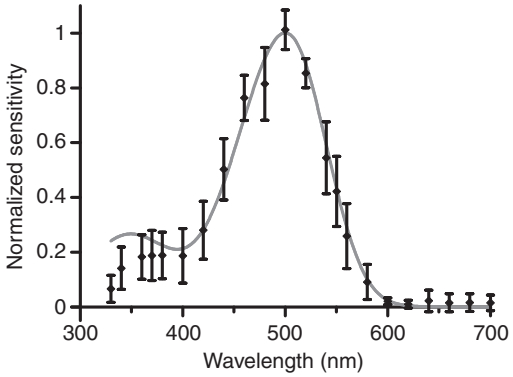


Fig. 5. Mean spectral sensitivity function for all *M. genalis* photoreceptors recorded. Grey line, a rhodopsin template with a $\lambda_{max}$ of 500 nm (from Govardovskii et al., 2000). Data points are means ± s.d.

increase in amplitude and a decrease in duration and latency (compare $I$=–1.8 with $I$=–1.0 in Fig. 3A). In the example shown in Fig. 3A, all but the first spike-like potentials disappeared from the response at high-intensity stimulation ($I$=0). However, partial light adaptation elicited by repeated application of bright light flashes (~30 applications at 1 s intervals) often led to the recurrence of multiple spike-like potentials.

Physiological responses to 'lights off' were not strongly marked in any recording. Fast rebound hyperpolarizing off transients, such as those observed in dragonfly ocellar photoreceptors (Chappell and Dowling, 1972; van Kleef et al., 2005), were likewise not observed in any recording. Photoreceptor membrane potential typically returned to the initial resting membrane potential within the space of 1 to 2 s post-stimulus (Fig. 3B). Intensity-response and spectral sensitivity functions described below were determined using a 15 s inter-stimulus interval, to ensure cells remained in the dark-adapted state as completely as possible without extending recording time beyond feasible limits.

Overall, we found wide variation in response waveform between cells from the same preparation, between cells from different preparations and in the same cell under different stimulus conditions. However, responses from the same cell under identical conditions were consistently reproducible: little variation was observed between the responses obtained with repeated exposures to the same stimulus. In some insect ocelli, information processing is wavelength dependent. In the honeybee (Goldsmith and Ruck, 1958) and dragonfly (Chappell and DeVoe, 1975; van Kleef et al., 2008), the response waveform depends not only on intensity, but also on the wavelength of stimulation. In *M. genalis* ocellar photoreceptors, we found no evidence for differences in response waveform that were attributable to differences in stimulus wavelength. A response waveform obtained by stimulation at one wavelength could be reproduced by stimulation at any other wavelengths, provided that the intensity was sufficient to produce a response of equal amplitude.

### Intensity-response functions

The absolute sensitivity and dynamic range of 13 photoreceptors was investigated by measuring intensity-response functions to monochromatic stimulation at 500 nm (Fig. 4). Absolute sensitivity varied widely between photoreceptors. Using a 1 mV response as the test criterion, absolute thresholds lay between $4.4\times10^{9}$ and $2.0\times10^{11}$ photons cm$^{-2}$ s$^{-1}$, a range of nearly 2 log units.

Although the location of absolute threshold varied widely between cells, a common feature appeared to be the wide dynamic range of response. Saturation was not achieved in any recording even with the brightest monochromatic stimulus possible in our setup; however, this was likely due to the fact that the receptive fields of the photoreceptors are extremely wide (because of very underfocused optics) and the small point source used for stimulation filled only a minute fraction of this field. From the slope of the curves in Fig. 4 we can establish that, even in the least sensitive cells recorded, dynamic range must greatly exceed 2 log units. For the most sensitive cells recorded, dynamic range exceeds 3.5 log units. Intensity-response functions taken from a single highly sensitive photoreceptor, using white light rather than monochromatic light, indicate that the dynamic range of this cell lies in the order of 4 log units (Fig. 6). Similarly wide dynamic ranges have been described in the ocellar photoreceptors of the dragonfly (Chappell and Dowling, 1972) and locust (Simmons, 1995).

### Spectral sensitivity

The maximum spectral sensitivity ($\lambda_{max}$) of all nine photoreceptors tested was located at ~500 nm (range 480–510 nm). The majority of photoreceptors recorded had spectral sensitivity functions that were slightly narrower than a single rhodopsin template with a $\lambda_{max}$ of 500 nm (Govardovskii et al., 2000), except in the UV (β-band) regions where sensitivity was typically much lower than predicted (Fig. 5). A small number of cells had especially broad spectral sensitivity functions, with particularly high sensitivity to wavelengths between 400 and 460 nm (sometimes forming a second peak at 460 nm). It is not known whether these broad sensitivity profiles represent a true physiological response or whether they are an artefact of the recording process.

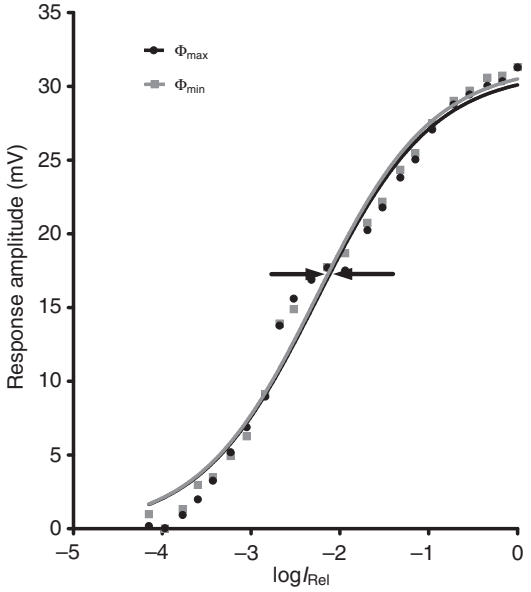


Fig. 6. Intensity-response functions at two orthogonal *e*-vector orientations. Intensity responses were measured with a linear polarising filter oriented to a position inducing maximal response ($\Phi_{max}$) and again after rotating the filter by 90 deg ($\Phi_{min}$). The degree of polarisation sensitivity is indicated by the amount of lateral shift ($\delta$ in log units) between the linear slopes of the two curves (centred at arrows). The high degree of overlap indicates this photoreceptor is not sensitive to the *e*-vector orientation of polarised light.

### Polarisation sensitivity

Polarisation sensitivity (PS) was assessed by measuring intensity-response functions to flashes of white light taken with a linear polarising filter in the light path oriented to a position deemed to give maximal response ($\Phi_{max}$), and again with the filter rotated by 90 deg ($\Phi_{min}$) (Greiner et al., 2007). PS is given by $10^{\delta}$, where $\delta$ is the difference (in log units) between the half-maximum responses of the two intensity-response functions (arrows in Fig. 6). In all photoreceptors tested, the intensity-response functions taken at $\Phi_{max}$ and $\Phi_{min}$ showed a very high degree of overlap, indicating that the photoreceptors were not polarisation sensitive ($\delta \approx 0$, therefore PS$\approx$1).

Complete intensity-response functions at $\Phi_{max}$ and $\Phi_{min}$ were only determined from three photoreceptors. However, many more cells were tested for polarisation sensitivity by manually rotating a polarising filter while observing responses to pulses of white light. In no case did we ever observe a change in response waveform or amplitude that was attributable to a change in *e*-vector orientation.

### Impulse responses

Dark-adapted photoreceptor temporal dynamics were investigated by recording impulse-response functions to brief flashes of dim light. The mean impulse response of six photoreceptors is shown in Fig. 7A. Time-to-peak ($\tau_p$) was typically in the order of 36 ms (range 32.6–44.7 ms), with half-widths ($\Delta t$) usually between 25 and 36 ms (range 24.6–58.8 ms). In general, latency and rise time varied little between all cells tested, but large variation was observed in the rate of return to baseline.

Temporal dynamics are best described by a frequency-response function that gives the power spectra of the cell to every frequency in its operational range. We obtained frequency responses by Fourier transforming the impulse-response functions (Fig. 7B). The frequency at which the signal power falls to 50% of its maximum (the corner frequency) provides a good comparative indicator of the temporal coding properties of the photoreceptor (Laughlin and Weckström, 1993). Corner frequencies of the photoreceptors typically lay between 4.2 and 6.8 Hz (range 4.2–10.6 Hz).

## DISCUSSION

In the present study we provide a comprehensive description of the internal structure of the ocellar lenses and retinae of *M. genalis*, and the physiological properties of the median ocellar photoreceptors. These results provide the foundation for further investigations into the functional roles of the ocelli. It should be noted that physiological responses were obtained from median ocellar photoreceptors only; it is possible that the physiological properties of lateral ocellar photoreceptors differ from those described here.

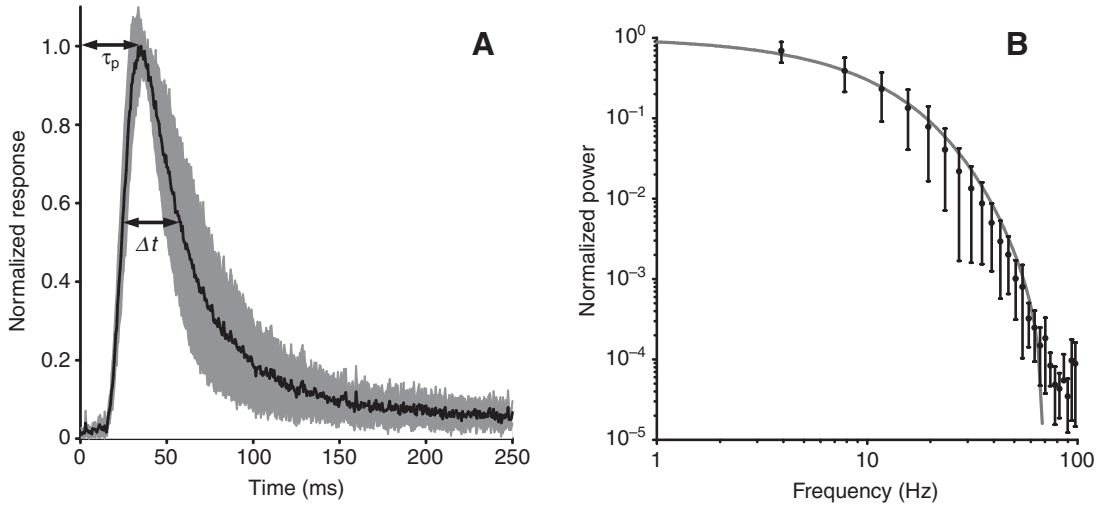


Fig. 7. Impulse and frequency responses of *M. genalis* ocellar photoreceptors. (A) Mean impulse response (black line) and standard deviation (grey fill) measured from six ocellar photoreceptors. Impulse responses were elicited by stimulation with a dim light flash delivered at time=0 ms. Data points were collected every 0.5 ms (sampling frequency of 2000 Hz). Mean time-to-peak ($\tau_p$) was 36.0 ms; mean half-width ($\Delta t$) was 36.4 ms. (B) Mean ± s.d. frequency response of six ocellar photoreceptors, as determined by Fourier transformation of their impulse-response functions. The grey line is an exponential curve fitted to the mean responses.

### Morphology and field of view

Warrant et al. previously investigated the optics and morphology of the median ocellus of *M. genalis* (Warrant et al., 2006). They found that, although the outer lens surface of the lens was strongly curved, the refractive power of the lens was not sufficient to bring parallel rays of light into focus on the retina. Warrant et al. did not describe the shape of the retina, but did state that it is directly attached to the inner lens surface (Warrant et al., 2006).

Using a combination of serial sectioning and reconstruction, we add to the previous study a comprehensive three-dimensional description of the internal structure of both the median and lateral ocelli. We found that the inner lens surfaces and retinae are of complex and non-uniform shapes. In the median ocellus, the bulk of the lens and retina project dorsally, resulting in a more ventral visual field centre than that predicted by external observation. As in many insects, the median ocellus also appears slightly bilobed (Fig. 2), which may reflect its development from two ocellar rudiments (Wheeler, 1936; Goodman, 1981).

The internal structure of the lateral ocellus is also non-uniform. Both the lens and retina are thickest along the medial-most aspect, especially at the dorsomedial extreme, where a large swelling of the retina occurs (Fig. 2, supplementary material Fig. S1). Cross-sections through the lateral ocelli of the honeybee *Apis mellifera* reveal a similar structure (W. Ribi, E.J.W. and J. Zeil, in preparation). This shape bears similarities to the lateral ocellus of the dragonfly, where both the inner surface of the lens and its associated retina are divided into dorsal and ventral regions (Berry et al., 2007c). Rhabdoms in the dorsal retina of the dragonfly lateral ocelli are longer and located much closer to the focal point of the lens than rhabdoms of the ventral retina. Berry et al. (Berry et al., 2007c) concluded that the two regions of the retina have different functions: the more sensitive dorsal retina is optimally adapted for resolving the horizon whereas the less sensitive ventral retina is adapted for receiving an underfocused image from the sky. It is possible that the lateral ocelli of bees represent a less extreme version of the dragonfly lateral ocelli, in that the most sensitive and best focused photoreceptors in the lateral ocelli of *M. genalis* are those with the most ventral and lateral view.

Warrant et al. (Warrant et al., 2006) also described the cross-sectional structure of the median ocellus retina, which they gave as containing a somewhat disorganised array of rhabdoms, each formed by the fusion of two adjacent rhabdomeres with parallel microvilli. We confirm the results of the earlier study here, but find that the elongated rhabdoms are oriented in a loosely radial pattern around the lens. Rhabdom shape and orientation is more tightly ordered in the distal retina: near the proximal limit of the retina rhabdom shape and orientation becomes increasingly irregular.

The fine structure of the retina of *M. genalis* also bears similarities to that of the honeybee. Toh and Kuwabara described the ocelli of the worker honeybee as consisting of ~800 elongated rhabdoms with parallel microvilli, eight large diameter second-order neurons (L-neurons) and an indeterminate number of smaller diameter second-order neurons (Toh and Kuwabara, 1974). Each retinula cell repeatedly contacts a subset of the eight L-neurons, and convergence ratios of 100:1 have been estimated for these neurons (Toh and Kuwabara, 1974). We found that total rhabdom number is lower in *M. genalis* (150–200), but the rhabdoms are larger: 17.5×1.3 μm in *M. genalis* (Warrant et al., 2006) as opposed to 10×1 μm in the honeybee (Toh and Kuwabara, 1974). From cross-sections of the ocelli of *M. genalis*, we estimate that at least 7–8 L-neurons (axon diameters of 10–20 μm) innervate each ocellus, although quantification of the exact number is difficult in this species because of the very close association of the three ocellar nerves to each other and to the brain. Because total rhabdom number is lower in *M. genalis* than in the honeybee, it is likely that convergence ratios in the former are correspondingly lower. This is an interesting finding given that higher convergence ratios are typically associated with improved sensitivity (Toh and Kuwabara, 1974; Goodman, 1981; Patterson and Chappell, 1980). It appears that in *M. genalis* ocelli, total rhabdom number has been sacrificed in favour of increased rhabdom size.

### Ocellar optimisations for low light vision in the rainforest understory

Wilson proposed that many prominent features of the ocelli – such as their underfocused optics, wide fields of view, spectral sensitivities and direct connection to wing motor centres – may be understood if they are considered to be optimised intensity detectors used for correcting deviations from course during flight (Wilson, 1978). In such a system, the underfocused nature of the lenses as well as a wide field of view ensure that confounding spatial details such as trees and clouds have minimal impact on the intensity measured by the ocelli (Wilson, 1978). However, in contrast to honeybees, locusts and dragonflies, which are active in bright or open spaces, *M. genalis* is active at very low light levels in a visually cluttered environment where the horizon is not clearly visible. What features of *M. genalis*'s ocelli are adapted to life in the dim understory of a rain forest?

#### Absolute sensitivity and temporal resolution

The most difficult task of any visual system operating under low-light conditions is to catch sufficient photons to generate a reliable visual signal (Theobald et al., 2006). We may therefore expect several adaptations designed to improve sensitivity in the ocelli of *M. genalis*. The large size of the ocellar lens, in combination with the large volume of the rhabdoms, enhances the light trapping ability of the ocellus (Warrant et al., 2006). The absolute sensitivity of *M. genalis* ocellar photoreceptors recorded here varied widely; taking the lowest value encountered as the upper limit of the system yields a sensitivity of $4\times10^{9}$ photons $cm^{-2}\,s^{-1}$. From comparison to previous experiments using a stimulating apparatus similar to that used in the present study (a point light source of ~0.3 deg aperture), we found that *M. genalis* ocellar photoreceptors are: (1) considerably more sensitive than those in dragonfly ocelli, which approach threshold at ~$10^{11}$ photons $cm^{-2}\,s^{-1}$ (Chappell and Dowling, 1972; Stange, 1981); and (2) approximately equally as sensitive as photoreceptors in locust ocelli (Simmons, 1995) or second-order neurons of honeybee ocelli (Baader, 1989), which reach threshold at $10^{9}$–$10^{10}$ photons $cm^{-2}\,s^{-1}$. However, we may expect ocellar second-order neurons to have substantially greater sensitivity than the photoreceptors, because of high convergence ratios and because the connecting synapse operates with very high gain (Simmons, 1995; Simmons, 2002). Indeed, in dragonflies, the second-order neurons have been shown to be ~2 log units more sensitive than the photoreceptors (Chappell and Dowling, 1972). In locust second-order ocellar neurons, Wilson gives absolute sensitivity values of $10^{7}$ photons $cm^{-2}\,s^{-1}$ (Wilson, 1978), making these neurons sufficiently sensitive to produce saturated responses upon axial exposure to the full moon. Thus, although the absolute sensitivity value of $10^{9}$ photons $cm^{-2}\,s^{-1}$ given here for *M. genalis* compares favourably to other ocellar photoreceptors, we expect that this value does not represent the lower limit for the ocellar system.

In *M. genalis* ocelli, enhanced sensitivity has likely been gained at the expense of temporal resolution. In a comparative study across

several families of Diptera, Laughlin and Weckström found that compound eye photoreceptors of slow-flying nocturnal species tended to be slow but sensitive (dark-adapted corner frequencies of 7–11 Hz) whereas photoreceptors from fast-flying diurnal species tended to be fast but relatively insensitive (dark-adapted corner frequencies of 12–25 Hz) (Laughlin and Weckström, 1993). With corner frequencies generally in the order of 4.2–6.8 Hz, the ocellar photoreceptors of *M. genalis* are typically slower than the slowest compound eye photoreceptors recorded by Laughlin and Weckström (Laughlin and Weckström, 1993), and are also much slower than the second-order neurons of honeybee ocelli (corner frequencies of 17–32 Hz) (Baader, 1989). However, the dark-adapted photoreceptors of the compound eyes of *M. genalis* have similar corner frequencies (Frederiksen et al., 2008), indicating that temporal resolution has been sacrificed in favour of greater sensitivity in both the ocelli and the compound eyes.

### Spectral sensitivity

The ocelli of most insects contain two or three visual pigments: one with peak sensitivity to UV light and additional pigments with peak sensitivity to blue or green light (Goldsmith and Ruck, 1958; Chappell and DeVoe, 1975; Hu et al., 1978; Wilson, 1978). Rather unusually, we did not find a short-wavelength visual pigment in the ocelli of *M. genalis*. All cells we recorded were maximally sensitive to light of ~500 nm wavelength (Fig. 5).

Wilson proposed that UV sensitivity is strongly beneficial for a visual system involved in correcting body attitude, because the contrast between the sky and ground is especially strong in the UV range (Wilson, 1978). Why don't the ocelli of *M. genalis* utilise the high-contrast UV signal? One possible explanation is that in dense rainforests, UV is strongly absorbed by overhead foliage (Endler, 1993). Longer wavelengths, however, are likely to be strongly reflected, and downwelling green light may provide a strong intensity gradient that can be used for determining which way is up. Another possible explanation is that most naturally lit nocturnal scenes contain substantially more green photons than UV photons (Johnsen et al., 2006); longer wavelength visual pigments are therefore more likely to maximise photon catch at night. In this regard, UV-insensitive ocelli have also been described in the nocturnal cockroaches *Periplaneta americana* and *Blaberus craniifer*, which possess only a single visual pigment with peak sensitivity at 500 nm (Goldsmith and Ruck, 1958). Cockroaches, however, are not strong fliers; utilisation of the high contrast difference between the sky and the ground in the UV range may be of less importance in these animals and their ocelli may serve functions other than attitude stabilisation.

### Polarisation sensitivity

Given that the elongated rhabdoms of *M. genalis* ocelli are formed by the fusion of two photoreceptors with microvilli oriented in a parallel direction, Warrant et al. suggested the ocelli of *M. genalis* might extract compass information by detecting the *e*-vector orientation of skylight visible through gaps in the rainforest canopy overhead (Warrant et al., 2006). Here, we tested polarisation sensitivity directly by comparing responses to linearly polarised light of different *e*-vector orientations. We found no evidence for the presence of polarisation sensitivity in these cells.

Indeed, the complete lack of even a small degree of polarisation sensitivity begs an explanation. Closer analysis of the rhabdoms reveals two factors that may partially account for this lack. First, cross-sections reveal that individual rhabdoms, especially more proximally, are often worm-like in appearance rather than straight bars (Fig. 2). This would lead to a reduction (or elimination) of polarisation sensitivity due to variable orientations of microvilli in each rhabdom. Second, rhabdoms are not aligned in a common direction, but instead form a roughly radial pattern around the centre of the lens. If many photoreceptors are coupled together, as is known to occur in dragonfly ocelli (Dowling and Chappell, 1972), then strong polarisation sensitivity in one rhabdom may be degraded by pooling from neighbouring photoreceptors that respond maximally to different *e*-vector orientations.

### Physiological variation

Overall, we found that the physiological responses of *M. genalis* ocellar photoreceptors exhibited markedly wide variation, especially in their response waveform to light pulses (Fig. 3) and absolute sensitivity (Fig. 4). Additionally, responses to lights-on often included multiple spike-like potentials (Fig. 3). Fast phasic responses at the onset of a light stimulus are a common feature in ocellar photoreceptors (reviewed in Goodman, 1981), but multiple spike-like potentials like those observed here have not been previously described. Photoreceptors of the honeybee drone compound eye, however, are known to produce spikes (Baumann, 1968), and spike-like potentials have also been observed in the second-order neurons of the honeybee ocelli (Guy et al., 1979). In the case of the latter, Milde describes L-neurons in the ocellar nerve of the honeybee as capable of switching between spiking and non-spiking states (Milde, 1981). The presence or absence of spikes is dependent on the state of the neuron, the polarity and intensity of stimulation used and (potentially) the quality of the recording electrode (Milde, 1981). It is possible that the spike-like potentials observed in the ocellar photoreceptors of *M. genalis* reflect similar physiological features, or that the potentials are, in fact, generated by second-order neurons in a particular state and then back-propagated to the photoreceptors through the complex reciprocal synapses of the ocellar plexus (Dowling and Chappell, 1972; Toh and Kuwabara, 1974). Interestingly, the compound eye photoreceptors of another nocturnal insect, the cockroach *P. americana*, are also known to produce spike-like potentials in addition to graded responses (Weckström et al., 1993). Heimonen et al. recently demonstrated that these are generated from within the photoreceptor axon whereas the graded component of response is generated in the cell soma (Heimonen et al., 2006). The observed response waveform is thus a function of recording site: recordings from the soma are dominated by strong graded responses, with weakly back-propagated spikes also visible; recordings from the axon consist of large-amplitude spikes and relatively weak graded responses. It is quite possible that such a correlation also exists in *M. genalis*, but this could not be verified here because of the short length of the photoreceptors and because the dark pigment sheathing the retina obscures visibility.

Heimonen et al. also described unusually wide variation in response waveform, rate of adaptation, absolute sensitivity, angular sensitivity and signal-to-noise ratio in the cockroach compound eye photoreceptors (Heimonen et al., 2006). They showed that the large variability in the physiological properties of the photoreceptors, in combination with a spike coding scheme, represents a strategy for optimising vision in low light. Using parameters obtained from their physiological experiments, they generated a theoretical model of a second-order cell receiving input from 12 photoreceptors. The output of the simulated second-order neuron followed a simulated light source most closely when the physiological parameters of the photoreceptors varied widely, i.e. population coding from a pool of diverse photoreceptors improves robustness at low intensities, when light signals are inherently unreliable. Given the similarities in

anatomical and physiological variability between *P. americana* and *M. genalis*, as well as the presence of 'spiking' photoreceptors, it is tempting to suggest that the response variability observed in nocturnal bee ocellar photoreceptors represents a similar adaptation for improved detection at low light levels.

In a review on the form and function of the ocelli across insects, Mizunami classified ocelli into three classes: (1) the 'cockroach type', characterised by very high sensitivity but low speed; (2) the 'bee type', characterised by high speed but lower sensitivity; and (3) the 'locust type', where both sensitivity and speed are emphasised (Mizunami, 1995). Given the adaptations for sensitivity, the slow temporal dynamics and the lack of UV sensitivity, it appears that the ocelli of *M. genalis* may have more in common with the ocelli of cockroaches than with those of other bees. Despite stark differences in lifestyle and habitat, both species confront the same problems associated with vision in dim light environments and appear to have convergently evolved similar mechanistic solutions for 'seeing in the dark'.

## ACKNOWLEDGEMENTS

This work would not have been possible without the help of Drs Rikard Frederiksen, Eva Kreiss and Henrik Malm, who assisted with the collection of bees and various other administrative and technical matters. We would also like to thank the staff of the Smithsonian Tropical Research Institute, in particular Dr Simon Tierney for his extensive help. We are also grateful to the Autoridad Nacional del Ambiente of the Republic of Panama for permission to export bees (permit no. SEX/A-25-09). We would like to thank the Air Force Office of Scientific Research (contracts FA 4869 and FA8655-07-C-4011), the Royal Physiographic Society of Lund and the Swedish Research Council for funding this work.

## REFERENCES

**Baader, A.** (1989). Sensitivity of ocellar interneurons of the honeybee to constant and temporally modulated light. *J. Neurobiol.* **20**, 519-529.
**Baumann, F.** (1968). Slow and spike potentials recorded from retinula cells of the honeybee drone in response to light. *J. Gen. Physiol.* **52**, 855-875.
**Berry, R., Stange, G., Olberg, R. and van Kleef, J.** (2006). The mapping of visual space by identified large second-order neurons in the dragonfly median ocellus. *J. Comp. Physiol. A* **192**, 1105-1123.
**Berry, R. P., Stange, G. and Warrant, E. J.** (2007a). Form vision in the insect dorsal ocelli: an anatomical and optical analysis of the dragonfly median ocellus. *Vision Res.* **47**, 1394-1409.
**Berry, R. P., Warrant, E. J. and Stange, G.** (2007b). Form vision in the insect dorsal ocelli: an anatomical and optical analysis of the locust ocelli. *Vision Res.* **47**, 1382-1393.
**Berry, R., van Kleef, J. and Stange, G.** (2007c). The mapping of visual space by dragonfly lateral ocelli. *J. Comp. Physiol. A* **193**, 495-513.
**Chappell, R. L. and DeVoe, R. D.** (1975). Action spectra and chromatic mechanisms of cells in the median ocelli of dragonflies. *J. Gen. Physiol.* **65**, 399-419.
**Chappell, R. L. and Dowling, J. E.** (1972). Neural organization of the median ocellus of the dragonfly: I. Intracellular electrical activity. *J. Gen. Physiol.* **60**, 121-147.
**Cornwell, P. B.** (1955). The functions of the ocelli of *Calliphora* (Diptera) and *Locusta* (Orthoptera). *J. Exp. Biol.* **32**, 217-237.
**Dowling, J. E. and Chappell, R. L.** (1972). Neural organization of the median ocellus of the dragonfly. II. Synaptic structure. *J. Gen. Physiol.* **60**, 148-165.
**Endler, J. A.** (1993). The color of light in forests and its implications. *Ecol. Monogr.* **63**, 1-27.
**Frederiksen, R., Wcislo, W. T. and Warrant, E. J.** (2008). Visual reliability and information rate in the retina of a nocturnal bee. *Curr. Biol.* **18**, 349-353.
**Goldsmith, T. H. and Ruck, P. R.** (1958). The spectral sensitivities of the dorsal ocelli of cockroaches and honeybees: an electrophysiological study. *J. Gen. Physiol.* **41**, 1171-1185.
**Goodman, L. J.** (1981). Organisation and physiology of the insect dorsal ocellar system. In *Handbook of Sensory Physiology: Invertebrate Visual Centres and Behaviour*, VII/6C (ed. H. Autrum), pp. 201-286. Berlin, Heidelberg, New York: Springer.
**Govardovskii, V. I., Fyhrquist, N., Reuter, T., Kuzmin, D. G. and Donner, K.** (2000). In search of the visual pigment template. *Vis. Neurosci.* **17**, 509-528.
**Greiner, B., Ribi, W. A. and Warrant, E. J.** (2004a). Retinal and optical adaptations for nocturnal vision in the halictid bee *Megalopta genalis*. *Cell Tissue Res.* **316**, 377-390.
**Greiner, B., Ribi, W. A., Wcislo, W. T. and Warrant, E. J.** (2004b). Neural organisation in the first optic ganglion of the nocturnal bee *Megalopta genalis*. *Cell Tissue Res.* **318**, 429-437.
**Greiner, B., Ribi, W. A. and Warrant, E. J.** (2005). A neural network to improve dim-light vision? Dendritic fields of first-order interneurons in the nocturnal bee *Megalopta genalis*. *Cell Tissue Res.* **322**, 313-320.
**Greiner, B., Cronin, T. W., Ribi, W. A., Wcislo, W. T. and Warrant, E. J.** (2007). Anatomical and physiological evidence for polarisation vision in the nocturnal bee *Megalopta genalis*. *J. Comp. Physiol. A* **193**, 591-600.
**Guy, R. G., Goodman, L. J. and Mobbs, P. G.** (1979). Visual interneurons in the bee brain: Synaptic organisation and transmission by graded potentials. *J. Comp. Physiol. A* **134**, 253-264.
**Heimonen, K., Salmela, I., Kontiokari, P. and Weckström, M.** (2006). Large functional variability in cockroach photoreceptors: optimization to low light levels. *J. Neurosci.* **26**, 13454-13462.
**Homann, H.** (1924). Zum Problem der Ocellenfunktion bei den Insekten. *Zeitschrift für Vergleichende Physiologie* **1**, 541-578.
**Hu, K. G., Reichert, H. and Stark, W. S.** (1978). Electrophysiological characterization of *Drosophila* ocelli. *J. Comp. Physiol. A* **126**, 15-24.
**Johnsen, S., Kelber, A., Warrant, E., Sweeney, A. M., Widder, E. A., Lee, R. L., Jr and Hernández-Andrés, J.** (2006). Crepuscular and nocturnal illumination and its effects on color perception by the nocturnal hawkmoth *Deilephila elpenor*. *J. Exp. Biol.* **209**, 789-800.
**Kastberger, G.** (1990). The ocelli control the flight course in honeybees. *Physiol. Entomol.* **15**, 337-346.
**Kelber, A., Warrant, E. J., Pfaff, M., Wallén, R., Theobald, J. C., Wcislo, W. T. and Raguso, R. A.** (2006). Light intensity limits foraging activity in nocturnal and crepuscular bees. *Behav. Ecol.* **17**, 63-72.
**Kerfoot, W. B.** (1967). Correlation between ocellar size and the foraging activities of bees (Hymenoptera; Apoidea). *Am. Nat.* **101**, 65-70.
**Laughlin, S. B. and Weckström, M.** (1993). Fast and slow photoreceptors – a comparative study of the functional diversity of coding and conductances in the Diptera. *J. Comp. Physiol. A* **172**, 593-609.
**Leigh, E. G., Jr** (1999). *Tropical Forest Ecology: A View From Barro Colorado Island*. Oxford, New York: Oxford University Press.
**Michener, C. D.** (2000). *The Bees of the World*. Baltimore, MD: Johns Hopkins University Press.
**Milde, J.** (1981). Graded potentials and action potentials in the large ocellar interneurons of the bee. *J. Comp. Physiol. A* **143**, 427-434.
**Mizunami, M.** (1994). Information processing in the insect ocellar system: comparative approaches to the evolution of visual processing and neural circuits. *Adv. Insect Physiol.* **25**, 151-265.
**Mizunami, M.** (1995). Functional diversity of neural organization in insect ocellar systems. *Vision Res.* **35**, 443-452.
**Mote, M. I. and Wehner, R.** (1980). Functional characteristics of photoreceptors in the compound eye and ocellus of the desert ant, *Cataglyphis bicolor*. *J. Comp. Physiol. A* **137**, 63-71.
**Pan, K. C. and Goodman, L. J.** (1977). Ocellar projections within the central nervous system of the worker honey bee, *Apis mellifera*. *Cell Tissue Res.* **176**, 505-527.
**Parry, D. A.** (1947). The function of the insect ocellus. *J. Exp. Biol.* **24**, 211-219.
**Parsons, M. M., Krapp, H. G. and Laughlin, S. B.** (2006). A motion-sensitive neurone responds to signals from the two visual systems of the blowfly, the compound eyes and ocelli. *J. Exp. Biol.* **209**, 4464-4474.
**Parsons, M. M., Krapp, H. G. and Laughlin, S. B.** (2010). Sensor fusion in identified visual interneurons. *Curr. Biol.* **20**, 624-628.
**Patterson, J. A. and Chappell, R. L.** (1980). Intracellular responses of procion filled cells and whole nerve cobalt impregnation in the dragonfly median ocellus. *J. Comp. Physiol.* **139**, 25–39.
**Schuppe, H. and Hengstenberg, R.** (1993). Optical properties of the ocelli of *Calliphora erythrocephala* and their role in the dorsal light response. *J. Comp. Physiol. A* **147**, 143-149.
**Simmons, P.** (1980). A locust wind and ocellar brain neurone. *J. Exp. Biol.* **85**, 285-294.
**Simmons, P. J.** (1981). Synaptic transmission between second- and third-order neurons of a locust ocellus. *J. Comp. Physiol. A* **145**, 265-276.
**Simmons, P. J.** (1995). The transfer of signals from photoreceptor cells to large second-order neurones in the ocellar visual system of the locust *Locusta migratoria*. *J. Exp. Biol.* **198**, 537-549.
**Simmons, P. J.** (2002). Signal processing in a simple visual system: the locust ocellar system and its synapses. *Microsc. Res. Tech.* **56**, 270-280.
**Simmons, P. J. and Littlewood, P. M. H.** (1989). Structure of a tonically transmitting synapse between identified interneurones in the locust brain. *J. Comp. Neurol.* **283**, 129-142.
**Stange, G.** (1981). The ocellar component of flight equilibrium control in dragonflies. *J. Comp. Physiol. A* **141**, 335-347.
**Stange, G., Stowe, S., Chahl, J. and Massaro, A.** (2002). Anisotropic imaging in the dragonfly median ocellus: a matched filter for horizon detection. *J. Comp. Physiol. A* **188**, 455-467.
**Taylor, C. P.** (1981). Contribution of compound eyes and ocelli to steering of locusts in flight: I. Behavioural analysis. *J. Exp. Biol.* **93**, 1-18.
**Theobald, J. C., Greiner, B., Wcislo, W. T. and Warrant, E. J.** (2006). Visual summation in night-flying sweat bees: a theoretical study. *Vision Res.* **46**, 2298-2309.
**Theobald, J. C., Coates, M. M., Wcislo, W. T. and Warrant, E. J.** (2007). Flight performance in night-flying sweat bees suffers at low light levels. *J. Exp. Biol.* **210**, 4034-4042.
**Toh, Y. and Kuwabara, M.** (1974). Fine structure of the dorsal ocellus of the worker honeybee. *J. Morphol.* **143**, 283-305.
**van Kleef, J., James, A. C. and Stange, G.** (2005). A spatiotemporal white noise analysis of photoreceptor responses to UV and green light in the dragonfly median ocellus. *J. Gen. Physiol.* **126**, 481-497.
**van Kleef, J., Berry, R. and Stange, G.** (2008). Directional selectivity in the simple eye of an insect. *J. Neurosci.* **28**, 2845-2855.
**Warrant, E. J.** (2008a). Seeing in the dark: vision and visual behaviour in nocturnal bees and wasps. *J. Exp. Biol.* **211**, 1737-1746.
**Warrant, E. J.** (2008b). Nocturnal vision. In *The Senses: A Comprehensive Reference*, Vol. 2, Vision II (ed. T. Albright and R. H. Masland) (series ed. A. I. Basbaum, A. Kaneko, G. M. Shepherd and G. Westheimer), pp. 53-86. Oxford: Academic Press.

**Warrant, E. J., Kelber, A., Gislén, A., Greiner, B., Ribi, W. and Wcislo, W. T.** (2004). Nocturnal vision and landmark orientation in a tropical halictid bee. *Curr. Biol.* **14**, 1309-1318.
**Warrant, E. J., Kelber, A., Wallén, R. and Wcislo, W. T.** (2006). Ocellar optics in nocturnal and diurnal bees and wasps. *Arthropod Struct. Dev.* **35**, 293-305.
**Wcislo, W. T. and Tierney, S. M.** (2009). Behavioral environments and niche construction: the evolution of dim-light foraging in bees. *Biol. Rev* **84**, 19-37.
**Wcislo, W. T., Arneson, L., Roesch, K., Gonzalez, V., Smith, A. and Fernández, H.** (2004). The evolution of nocturnal behavior in sweat bees, *Megalopta genalis* and *M. ecuadoria* (Hymenoptera: Halictidae): an escape from competitors and enemies? *Biol. J. Linnean Soc.* **83**, 377-387.
**Weckström, M., Järvilehto, M. and Heimonen, K.** (1993). Spike-like potentials in the axons of nonspiking photoreceptors. *J. Neurophysiol.* **69**, 293-296.
**Wellington, W. G.** (1974). Bumblebee ocelli and navigation at dusk. *Science* **183**, 550-551.
**Wheeler, W. M.** (1936). Binary anterior ocelli in ants. *Biol. Bull.* **70**, 185-192.
**Wilson, M.** (1978). The functional organisation of locust ocelli. *J. Comp. Physiol. A* **124**, 297-316.